ENGINEER - Vol. LVIII, No. 04, pp. [93-104], 2025

DOI: https://doi.org/10.4038/engineer.v58i4.7720

Coupled Effects of Fire and Cyclic Loading on the Seismic Resilience of Steel Moment Resisting Frames

B.V.D.D. Tharaka, A.S. Gampalage, Y.P.K.M.W.N. Kanakarathna, J.A.S.C. Jayasinghe and S. Bandara

Abstract: Steel structures are significant in modern construction due to their high strength, durability and rapid construction. However, one of the primary vulnerabilities of steel is its performance under elevated temperatures. Therefore, degradation of properties can lead to large deformations, instability or even collapse of steel members during post-earthquake fire scenarios. Hence, understanding the thermo-mechanical behaviour of steel and evaluating the structural response under sequential earthquake and fire loading is critical for ensuring structural resilience. Both experimental and numerical approaches can be used to investigate structural behaviour. However, numerical analysis is often preferred due to the high cost and time consumption of experimental studies. A numerical model is developed in this study to assess the seismic performance of a 4-bay, 2-story hollow steel moment-resisting frame under the combined effects of fire and cyclic loading. A coupled Computational Fluid Dynamics (CFD) and Finite Element Method (FEM) simulation was used to analyse the fire development, thermal response and structural behaviour. Non-uniform fire scenarios were generated using *PyroSim* which is a graphical interface for the Fire Dynamics Simulator (FDS), while *ABAQUS* was employed for finite element analysis. Thermal data obtained from CFD simulations were mapped to the FE model using the *FDS2FEM* tool through the NSET-BNDF method enabling unidirectional coupling. Subsequent thermal and structural analyses were sequentially performed, with structural performance evaluated under lateral cyclic loading to represent seismic effects. The accuracy of the numerical model was verified through validation, and the parametric study was performed to assess the impacts of fire location and beam flexural stiffness on the seismic performance. The results indicated that fires located at columns adjacent to the cyclic loading point caused the most significant reductions in strength and ductility, with reductions of 9.8% and 15.09%, respectively. In contrast, fires directly at the cyclic loading point led to the smallest improvement in energy absorption capacity, measured at 10.01%. Additionally, increasing the flexural stiffness of the middle beam enhanced both strength and energy absorption capacity, while resulting in a slight reduction in ductility.

Keywords: Computational fluid dynamics; Finite element simulation; Fire simulation; Moment-resisting frame; Seismic response

1. Introduction

Steel is a widely used material in the construction of structures such as skyscrapers, bridges, industrial buildings, and stadiums due to its high strength, durability, versatility, design flexibility, and rapid construction capabilities [1]. However, its mechanical properties are significantly affected by elevated temperatures, which can lead to a reduction in strength and stability. In the event of a fire, this deterioration becomes critical, as it can compromise structural integrity, leading to failures such as buckling columns and sagging beams. Real-world incidents, such as the collapse of the World Trade Center (2001) and the Windsor Tower fire (2005), highlight the devastating effects of prolonged exposure to fire on steel structures [2,3].

Similarly, seismic forces generated during earthquakes can cause severe structural failures,

*Eng. **B.V.D.D. Tharaka**, AMIE(SL), B.Sc. Eng. (Hons) (Peradeniya), Department of Civil Engineering, Faculty of Engineering, University of Peradeniya.*
Email: e18353@eng.pdn.ac.lk
https://orcid.org/0009-0002-1684-6417
*Eng. **A.S. Gampalage**, AMIE(SL), B.Sc. Eng. (Hons) (Peradeniya), Department of Civil Engineering, Faculty of Engineering, University of Peradeniya.*
Email: e18109@eng.pdn.ac.lk
https://orcid.org/0009-0006-0737-2976
*Eng. **Y.P.K.M.W.N. Kanakarathna**, AMIE(SL), B.Sc. Eng. (Hons) (Peradeniya), Department of Civil Engineering, Faculty of Engineering, University of Peradeniya.*
Email: warshnirmani@gmail.com
https://orcid.org/0009-0005-4995-5515
*Eng. (Dr.) **J.A.S.C. Jayasinghe**, AMIE(SL), B.Sc. Eng. (Hons) (Peradeniya), M.Eng. (AIT), PhD. (Tokyo), Senior Lecturer in Department of Civil Engineering, University of Peradeniya, Sri Lanka.*
Email: supunj@eng.pdn.ac.lk
https://orcid.org/0000-0003-1054-9358
*Eng. (Dr.) **S. Bandara**, AMIE(SL), B.Sc. Eng. (Hons) (Peradeniya), PhD. (Swinburne), Lecturer in Department of Civil Engineering, University of Peradeniya, Sri Lanka.*
Email: sahan@eng.pdn.ac.lk
https://orcid.org/0000-0002-9090-7057

particularly in regions of high seismic activity. The 1995 Great Hanshin Earthquake in Kobe, Japan, serves as a significant example, where the collapse of buildings and highways was attributed to inadequate seismic design [4]. Another catastrophic event, the 2010 Haiti earthquake, shows the collapse of numerous structures due to poor construction practices [5]. 2011 Tohoku Earthquake in Japan not only caused widespread structural collapses but also triggered a devastating tsunami, further compounding the destruction [6].

The combined effect of both fire and earthquake can be more disastrous than the individual effect of each. However, the design of structures for fire and earthquake are typically conducted separately. For example, European standards use two distinct codes, one for fire design and another for earthquake design. In the design of steel structures for fire resistance, Eurocode 3 [7] is the relevant standard, while earthquake-resistant design is governed by Eurocode 8 [8] as outlined by Jiang et al. (2018) [9]. Apart from the design codes, there are experimental and numerical approaches for structural design under fire and earthquake. These approaches allow for the evaluation of structural performance under the combined effects of fire and earthquake.

Numerical simulation provides a practical and efficient means of studying the complex interactions between fire and cyclic loading on steel structures, offering detailed insights that are difficult to obtain through traditional laboratory experiments. There are several limitations of experimental approach mainly consuming more time and cost compared to numerical simulation. On the other hand, due to the limited data available, determining structural performance can be challenging, making it impractical to conduct a large number of experiments [9]. Therefore, an accurate numerical model validated against appropriate experimental results serves as a valuable alternative to address these limitations. The numerical approach includes fire modelling and coupled thermo-mechanical simulation.

Fire modeling can be approached through various methodologies, including nominal temperature-time curves [10], parametric temperature-time curves [11], zone models [12], localized fire models [13], and computational fluid dynamics (CFD) models [14]. Most studies consider fire using simplified fire models, such as the parametric fire curve, standard fire curve, and hydrocarbon fire curve, which do not account for the effects of real fire scenarios. [15,16]. The majority of research has considered standard fire curves for fire scenarios which can be summarized as ISO834 standard fire, ASTM E119 fire, and ASTM E1529 hydrocarbon fire as well and several studies have considered parametric fire curves in EN1991 1-2 for fire scenario [17,16]. Fire modelling using CFD-based tools such as FDS and its graphical user interface PyroSim allows the simulation of realistic fire scenarios [18,19,20]. In these advanced approaches, a Computational Fluid Dynamics (CFD) model is employed to replicate the fire scenario, accounting for environmental variables. Next, the thermal boundary conditions are extracted from the CFD model and integrated into the Finite Element (FE) model. Finally, a coupled thermal-mechanical FE simulation is conducted as outlined by Liu et al., (2021) [19]. The thermal results from the CFD simulations were first obtained and then used as input for the structural analysis. This step-by-step process defines the sequentially coupled analysis. Coupled thermal and structural analyses to assess seismic performance can be performed using FEM software, such as *ABAQUS*, *ANSYS*, *OpenSees*, and *LS-DYNA* [21,22]. Temperature or heat flux obtained from CFD model or standard fire curves is used as thermal boundary of fire scenario.

This study investigates the intricate interactions between fire and cyclic loads on steel moment-resisting frames to understand their effects on seismic performance. Utilizing a CFD-based fire modeling approach to simulate real fire scenarios, it focuses on evaluating seismic performance under the coupled scenario of fire and lateral cyclic loads, which represent seismic actions. This study explores multiple performance aspects, including seismic behavior, and establishes safe working conditions for steel moment-resisting frames subjected to the combined effect of fire and cyclic loads.

Research objectives include establishing a numerical methodology that emphasizes the degradation of steel's mechanical properties with temperature in a steel moment-resisting frame during a fire. It also seeks to conduct a parametric study of coupled thermo-mechanical analysis in moment resisting frame under different fire scenarios to evaluate seismic performance under combined fire and cyclic loading using the validated numerical model.

2. Numerical Modelling

Numerical modelling in this study was executed through three major steps, including fire modelling, thermal analysis, and structural analysis, as outlined in the sequence shown in Figure 1. The temperature data obtained from the CFD simulation serves as boundary conditions for the FE solver in a unidirectional coupling approach. This involved extracting the characteristic temperature, termed as adiabatic surface temperature, from the CFD solution and applying these values to the nodes of the FE model.

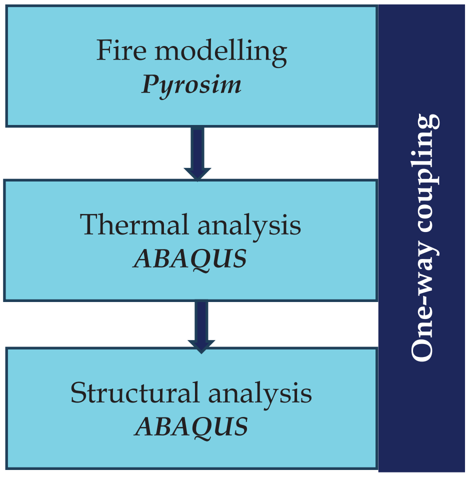

Figure 1 - Numerical modelling sequence

2.1 CFD Simulation Using FDS

This study employed Fire Dynamics Simulator (FDS) for CFD simulations. Low Mach number combustion equations were used on a rectilinear grid by the LES-based code FDS. In this study, *PyroSim* was used as the user interface of FDS which predicts smoke, temperature, carbon monoxide, and other substances during fires. Thermal radiation was calculated using the Finite Volume Method (FVM), while heat transfer to finite element solvers was handled via adiabatic surface temperatures. FDS computes solid heat conduction using a 1-D heat conduction equation.

The key fire modelling parameters in *PyroSim* include geometry, material properties, boundary conditions, heat release rate, and simulation settings.

Characteristic fire diameter (D^*) which is obtained from Eq. (1) [20], must be smaller than the mesh size to ensure an accurate representation of the fire scenario [19].

$$D^* = \left(\frac{Q}{\rho_\infty c_p T_\infty \sqrt{g}}\right)^{\frac{2}{5}} \quad \text{... (1)}$$

where Q is the fire size (kW), ρ_∞ is the ambient density, c_p is the specific heat of air, T_∞ is the ambient temperature and g is acceleration due to gravity. The ratio of the characteristic fire diameter (D^*) to the mesh cell size (δx), $D^*/\delta x$ defines the number of computational cells spanning the fire, ensuring adequate resolution in the simulation. Figure 2 illustrates the predicted adiabatic surface temperatures along a column during the FDS simulation conducted by Janardhan et al., (2022) [20].

2.2 Coupling Method Using *FDS2FEM*

FDS2FEM, a Fortran-based tool, integrates FDS data with *ABAQUS*, enabling sequential, unidirectional coupling of time and space dependent adiabatic surface temperatures (T_{AST}) from FDS to FE models. However, *FDS2FEM* has limitations, such as the inability to handle multiple-mesh geometries, non-uniform meshes, dynamic obstacle creation/removal, and fuel disappearance [23]. Two approaches are offered for mapping thermal boundary conditions: Node Set-Devices (NSET-DEVC) and Node Set-Boundary File (NSET-BNDF). In this study, NSET-BNDF was used for mapping time-dependent temperature and heat transfer values from FDS onto FE nodes as indicated in Figure 3. NSET-BNDF was chosen due to its ability to accurately handle large datasets and facilitate smooth integration between fire simulations and structural analysis [20].

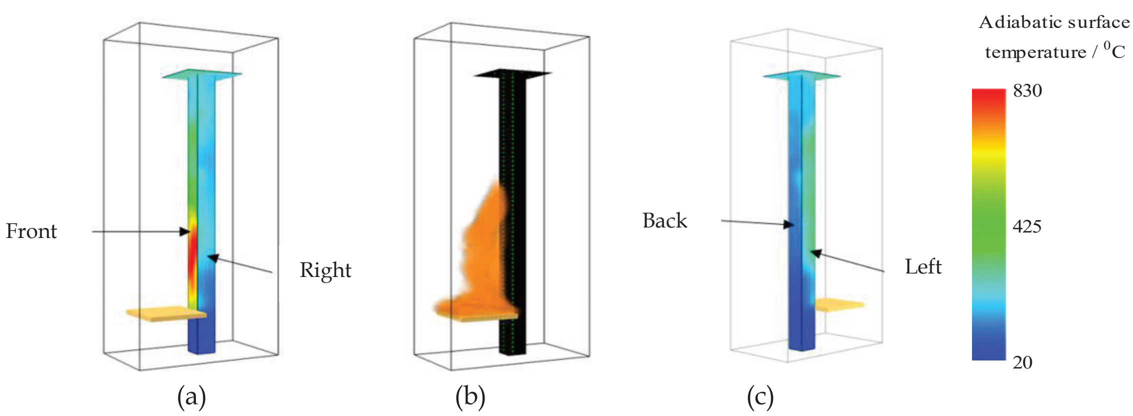

Figure 2 - FDS simulation results: (a) variation of adiabatic surface temperature on the front and right side of the columns (b) smoke view of the fire model and (c) variation of adiabatic surface temperatures on the back and left side of the columns [20]

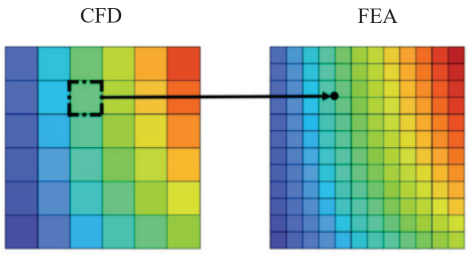

Figure 3 - Illustration of the Node Set-Boundary File (NSET-BNDF) mapping [20]

2.3 FE Analysis Using *ABAQUS*

Both thermal and mechanical analyses were conducted using the finite element software *ABAQUS*, which is capable of handling complex geometries, thermal conditions, and various constraints. For the thermal analysis, the DS4 type shell elements were employed, and the thermal field from the FDS model was mapped by importing the '.*inp*' file generated during the *FDS2FEM* procedure. The resulting data were then input into the mechanical analysis as a predefined field, taking into account the thermal conditions.

The mechanical analysis was conducted in *ABAQUS* by importing the thermal results as a '.*odb*' file into the model. The data were applied as a predefined field at the static general step to obtain the thermal deformations. In this analysis, the S4R type shell elements were utilized, ensuring that temperature-dependent material properties were considered throughout the simulation. Figure 4 indicates the meshed surface of the FE model and the predicted temperature distribution.

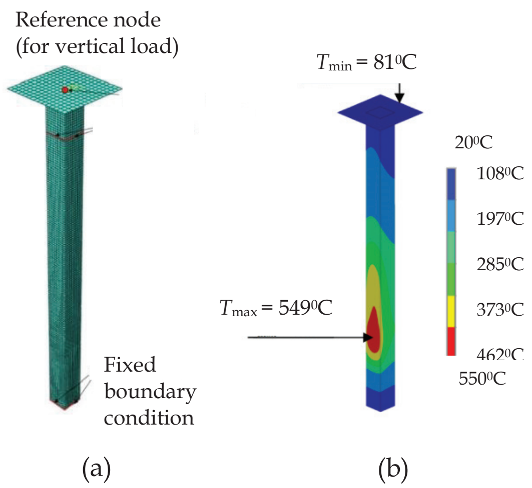

Figure 4 - FE model: (a) meshing mechanical boundary conditions and (b) resulting predicted temperature at 3600 s of fire [20]

2.3.1 Material Properties

Steel is highly temperature-sensitive, as its thermal properties change significantly, and it loses much of its mechanical strength when exposed to fire. The primary temperature-dependent material properties of steel, which include specific heat capacity, thermal conductivity, and thermal elongation, are shown in Figure 5. At elevated temperatures, the mechanical properties of steel undergo significant changes, resulting in a reduction in both its modulus of elasticity and the idealized stress-strain curves derived from Eurocode [7] stress-strain relationship compared to values at standard room temperature as indicated in Figure 6 [24]. These properties are well-documented in standards such as EN 1991-1-4:, 2005 [25] and EN 1993-1-2:, 2005 [7].

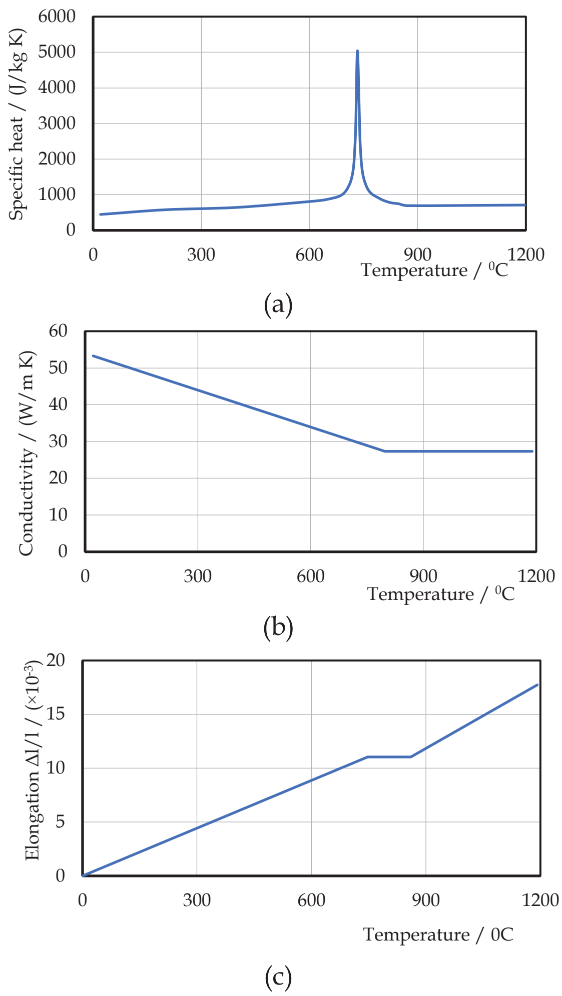

Figure 5 - Variation of thermal properties of steel: (a) specific heat (b) conductivity and (c) elongation of steel under elevated temperature [7]

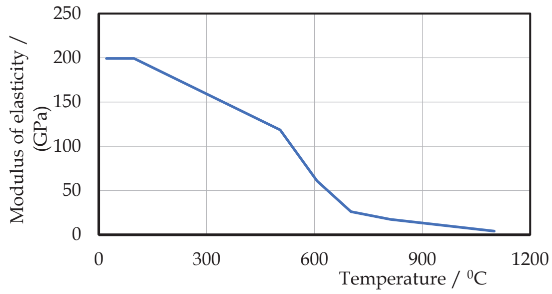

(a)

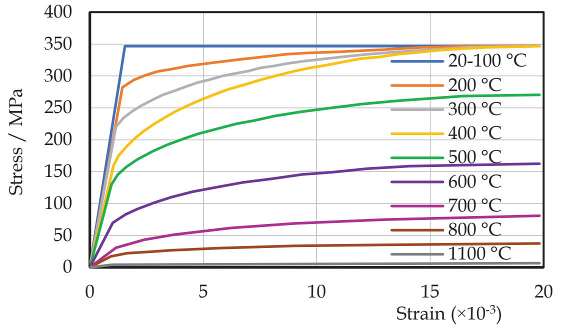

(b)

Figure 6 - Variation of mechanical properties of steel: (a) modulus of elasticity of steel under elevated temperature and (b) steel stress-strain curve under various temperatures [7]

3. Validation Study

The validation study involved each section discussed in the numerical modelling, as indicated in Figure 1. Validation of fire modelling and thermal analysis were conducted from the experiment test of Jiang et al. (2018) [9]. The structural analysis validation under cyclic loading was conducted for experiment test of Tateishi et al. (2008) [26].

3.1 Fire Model Validation

The FDS-based fire model was validated against the experimental setup involving a steel moment frame with four bays and two stories, with the fire location specified at the middle column, as depicted in Figure 7 [9]. Welded connections were utilized for beam-to-column connections. Rigid connections were established at the lower column ends through bolted connections fixed to the ground. The material of structural elements was steel 20 (National Steel Standardization Technical Committee of China 1999) [27], was quality carbon structural steel made in China. Loading was applied using metal lumps within steel boxes as indicated in Figure 8 and loading values are shown in Table 1. Out-of-plane displacement at the midpoint of each beam was restrained to maintain structural performance within the frame plane.

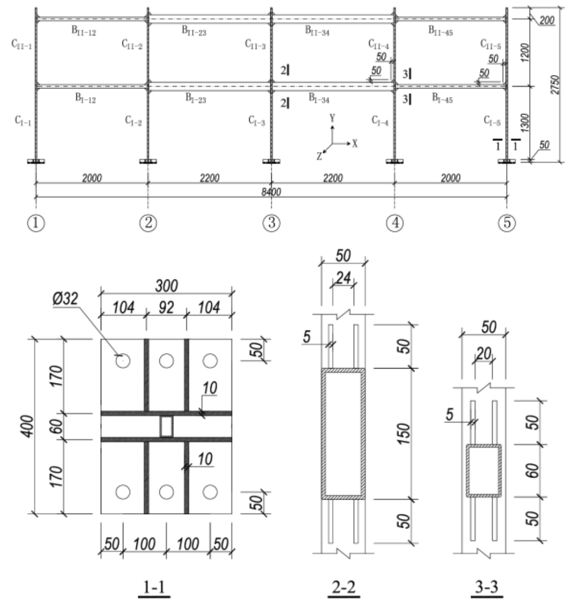

Figure 7 - Test frame details (*All dimensions are in millimetres*) [9]

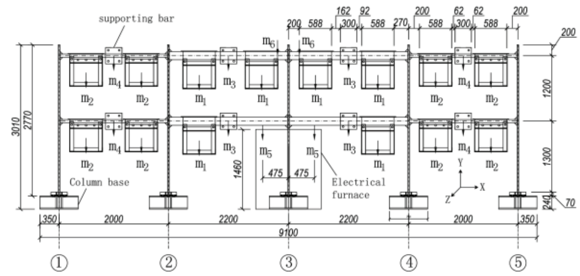

Figure 8 - Loading arrangement of test frame (*All dimensions are in millimetres*) [9]

Table 1 - Details of weights carried by the test frame [9]

Label	Value /(N)
m_1	2,910.0
m_2	1,760.7
m_3	701.3
m_4	766.0
m_5	73.9
m_6	74.0

PyroSim was used to carry out the validation simulations as FDS user interface. The wall temperature variation along the fire exposed column is shown in Figure 9. The wall temperature curves were obtained through *PyroSim* with a numerically converged mesh size of 50 mm. Temperature readings were taken at 220 mm, 490 mm, and 1020 mm heights from the base of the steel hollow column. A comparison between the FDS model results and the experimental data extracted from Jiang et al. (2018) [9] exhibited slight deviations indicated in Figure 10.

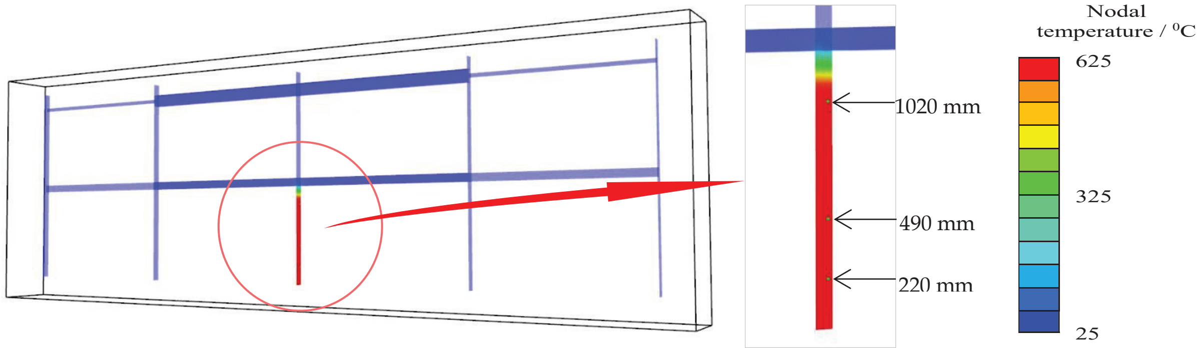

Figure 9 - FDS predicted wall temperature variation along the fire exposed column at peak temperature

After fire modeling using FDS, the coupling process was facilitated by *FDS2FEM*, and thermal analysis was subsequently performed in *ABAQUS*. The comparison between FDS and thermal analysis results shows that the temperature data transferred to *ABAQUS* closely correspond with the FDS output. This strong correlation confirms the accuracy of the data mapping process from FDS to FEM presented in Figure 10.

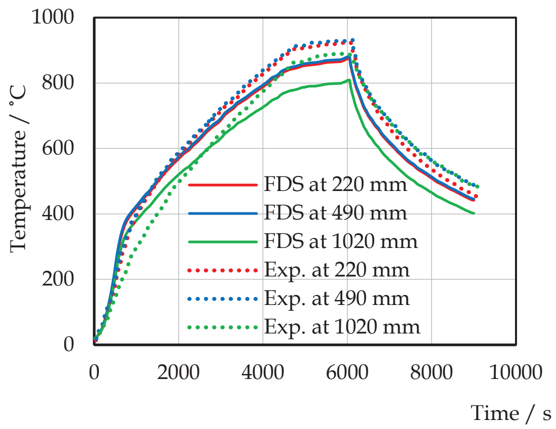

(a)

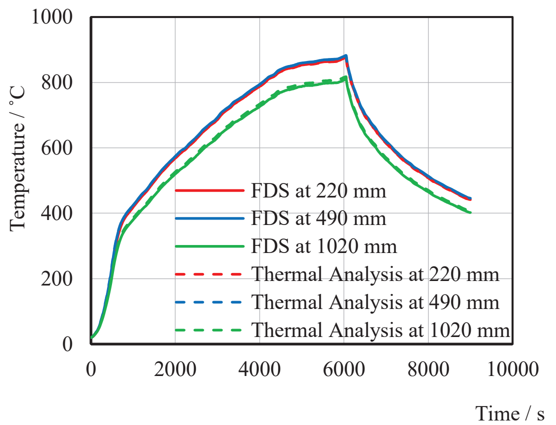

(b)

Figure 10 - Comparison of results: (a) FDS results vs experimental data [9] and (b) FDS results vs thermal analysis (FEM) results in fire exposed column

3.2 FE Model Validation Under Cyclic Loading

A preliminary study on cyclic loading was conducted based on the experimental tests by Tateishi et al. (2008) [26]. The configuration of column section and the cyclic loading pattern used in experiment are indicated in Figure 11. It is important to note that the lateral cyclic load pattern imposed on the column was characterized by symmetric cyclic loading, and the combined hardening rule was considered. Dimensions of the column section and the material properties of steel are indicated in Table 2. The steel column was modelled using *ABAQUS* software and the cyclic loading was applied on top of the column laterally and the non-dimensional bottom reaction and top displacements were plotted in the same graph as indicated in Figure 12. The cyclic envelope curves from the numerical and experimental results exhibited nearly identical trends with minimal deviations, confirming the model's capability to accurately simulate the structural response under cyclic loading.

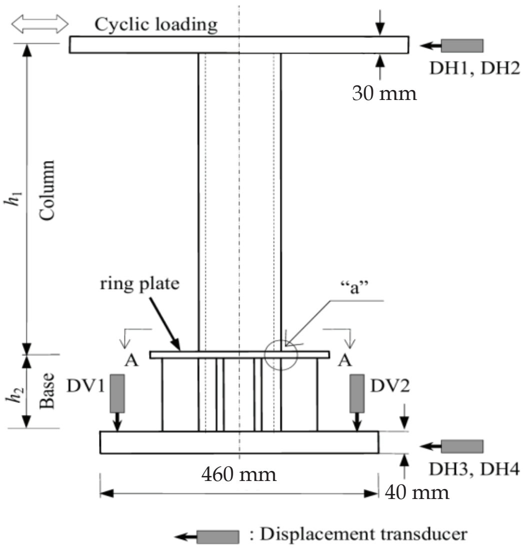

(a)

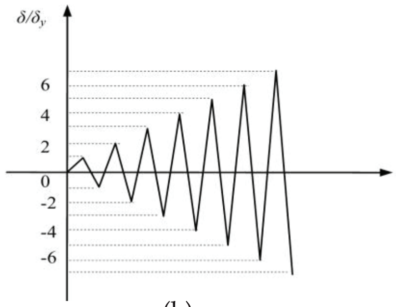

(b)

Figure 11 - Cyclic loading experimental set-up: (a) configuration of column section and (b) cyclic loading pattern [26]

Table 2 - Dimensions of the column and the material properties of steel [26]

Parameter	Value
Depth (h)	125 mm
Thickness (t)	12 mm
Sectional area (A)	161 mm
Height (h_1)	550 mm
Latter part height (h_2)	133 mm
Yield stress (f_y)	380 MPa
Young's modulus (E_s)	200 GPa
Ultimate stress (f_u)	531 MPa
Poisson's ratio	0.3

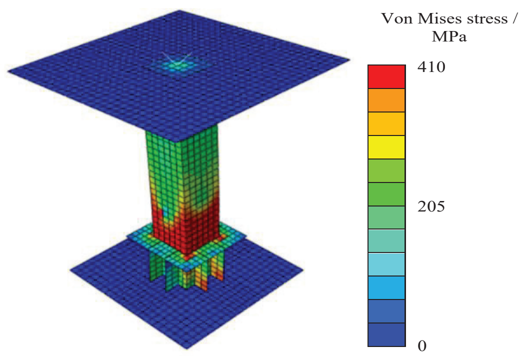

(a)

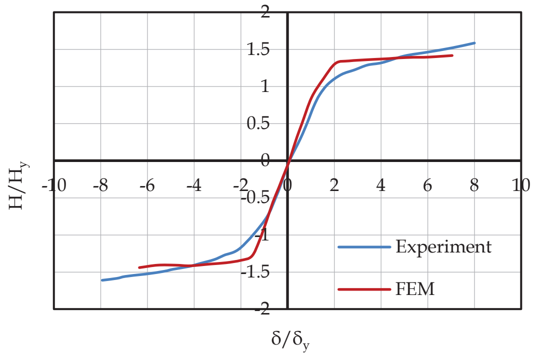

(b)

Figure 12 - Numerical results of cyclic loading: (a) Von Mises stress of column at 14th increment and (b) comparison of test results and numerical results [26]

4. Parametric Study

The parametric study was conducted to evaluate the seismic performance of a 4-bay, 2-story moment-resisting frame as indicated in Figure 13 with an electric furnace under combined fire and cyclic loading, following the test configuration described by Jiang et al. (2018) [9]. There were two main cases which the parametric study was conducted:

- Case 1: Change the location of fire, and
- Case 2: Change the middle bay beam flexural stiffness.

The fire was modelled in *PyroSim* based on the gas temperature curve from Jiang et al. (2018) [9], which reached steady state at 2920 seconds for both cases, as indicated in Figure 14.
Case 1 includes 5 sub cases where one of each bottom columns was subjected to fire which was represented as F1-F5 (F1 indicates fire at first column). For the Case 2 there were four sub cases where the middle bay beam flexural stiffness was varied which was represented by B1-B4.

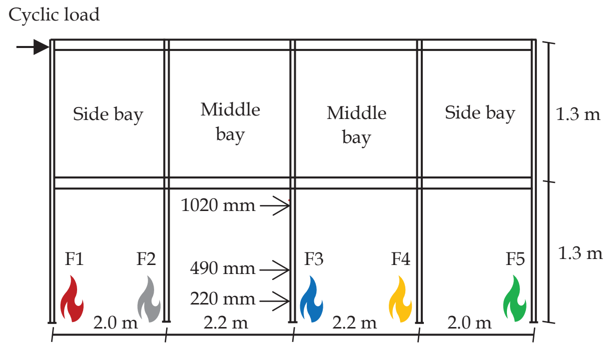

Figure 13 - Frame structure and the fire locations for the parametric study

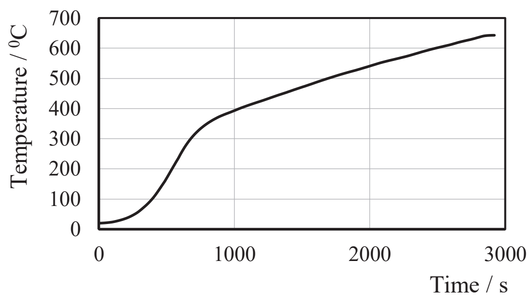

Figure 14 - Furnace gas temperature curve used for the parametric study [9]

The fire was applied at the 3rd column, which was the middle column in Case 2 and the cyclic load applied at top of first column as shown in Figure 13 which was a similar cyclic loading pattern as in validation study. The cross-section dimensions of each element in steel moment resisting frame, length × width × thickness, are indicated in Tables 3 and 4 for the two cases. The material properties of steel were considered as indicated in Seif et al., 2016 [28] and the loading on frame was considered as similar to loads in validation study [9].

Table 3 - Details of frame elements in Case 1

Column / (mm)	Middle bay beam / (mm)	Side-bay beam / (mm)
50 × 30 × 3	60 × 40 × 3.5	60 × 40 × 3.5

Table 4 - Details of frame elements in Case 2

Fire subcase	Column/ (mm)	Middle bay beam / (mm)	Flexural Stiffness (K)/ (MN/m)	Side-bay beam / (mm)
B1	50 × 30 × 3	150 × 50 × 5	46.1	60 × 40 × 3.5
B2		100 × 50 × 5	13.7	
B3		80 × 40 × 4	5.6	
B4		60 × 40 × 3.5	2.4	

The cyclic envelope curve would be obtained from the results of structural analysis which indicate variation of maximum top story displacement vs the total lateral force at bottom of columns for considered each case. In order to exclude the variation effect of geometry and boundary conditions, the response was obtained as normalized parameters using the yield load and yield displacement. For the parametric study, the yield displacement was obtained as 0.0236 m and yield load was 224.4 N. The resulting force and displacement were divided by yield load and yield displacement, respectively, and obtain normalized parameters. By considering the simulation mentioned in this section it would be possible to evaluate the seismic performance parameters which are ductility, strength, and energy absorption capacity.

4.1 Fire Modelling Results of Parametric Study

According to the parametric study, the fire modelling was conducted for Case 1 and Case 2. Since the same fire curve was used across all cases and only the fire-exposed column was heated, the results of fire modelling and thermal analysis (FEM) are same for all cases. Therefore, only one subcase (Case 1 subcase F3) was considered for indication of fire modelling and thermal analysis (FEM) as shown in Figure 15.

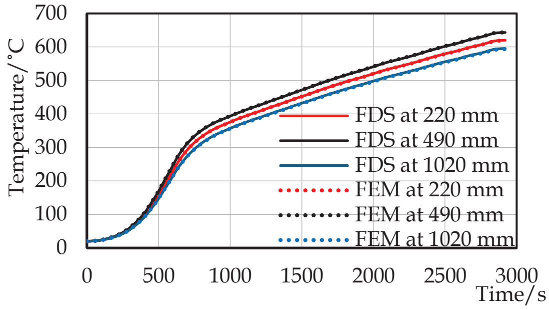

Figure 15 - Comparison of FDS results vs thermal analysis (FEM) results in fire exposed column

4.2 Structural Analysis Results of Case 1 in Parametric Study

The *ABAQUS* model, which received the thermal boundary conditions, was coupled with a mechanical analysis model that included cyclic loading. The structural analysis was conducted using shell elements. From results of structural analysis for Case 1, the normalized lateral load-lateral displacement envelope curves in fire condition as well as room temperature (25^{0}C) response and the cumulative energy absorption capacity curve were obtained as indicated in Figure 16.

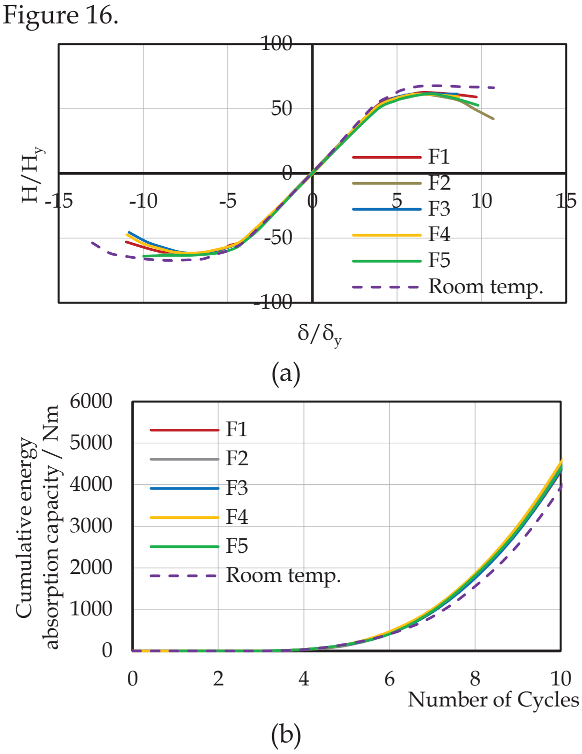

Figure 16 - Results of Case 1: (a) cyclic envelope curves and (b) cumulative energy curves

Considering the cyclic envelope curves under fire condition of Case 1, the maximum ductility, maximum strength and, by considering cumulative energy absorption capacity curves, the maximum accumulated energy absorption capacity was obtained as indicated in Figure 17. The percentage reduction or increment of seismic parameters of Case 1 was obtained as indicated in Table 5.

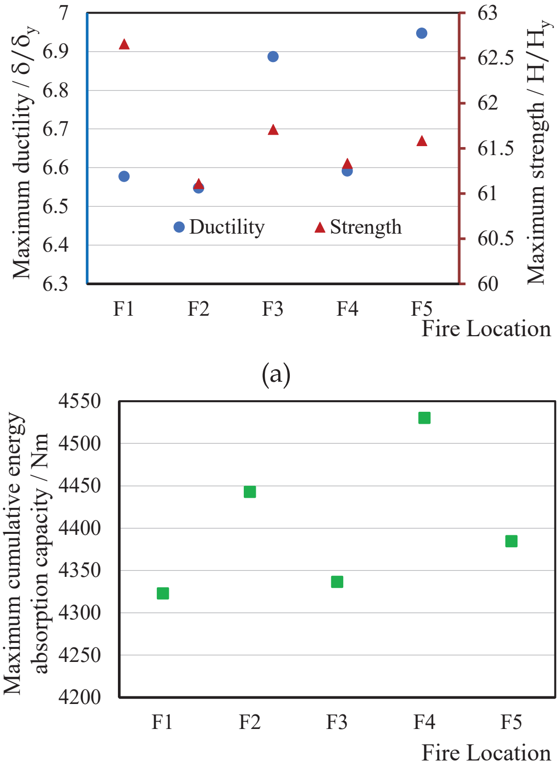

(b)

Figure 17 - Seismic parameters of Case 1: (a) maximum ductility and maximum strength variation and (b) maximum cumulative energy absorption capacity variation

Table 5 - Percentage variation of seismic parameters for Case 1

Fire subcase	Reduction (-) or incremental (+) percentage (%)		
	Maximum ductility	Maximum strength	Maximum cumulative energy absorption capacity
F1	-14.71	-7.52	+10.01
F2	-15.09	-9.80	+13.05
F3	-10.70	-8.92	+10.34
F4	-14.53	-9.47	+15.28
F5	-9.91	-9.10	+11.57

Lowest values of maximum ductility and strength were obtained in case F2 while the lowest maximum cumulative energy absorption capacity was obtained in case F1 according to Figure 17. When considering the percentage reduction of maximum ductility and strength, case F2 indicates the highest reduction percentage compared to the room temperature response. Maximum cumulative energy absorption capacity was increased compared to room temperature response and lowest increment was obtained in case F1.

4.3 Structural Analysis Results of Case 2 in Parametric Study

Using a similar procedure as discussed in Section 4.2, the structural analysis results were obtained for the Case 2. The normalized lateral load-lateral displacement envelope curves in fire condition as well as room temperature (25^{0}C) response and the cumulative energy absorption capacity curve were obtained as indicated in Figure 18.

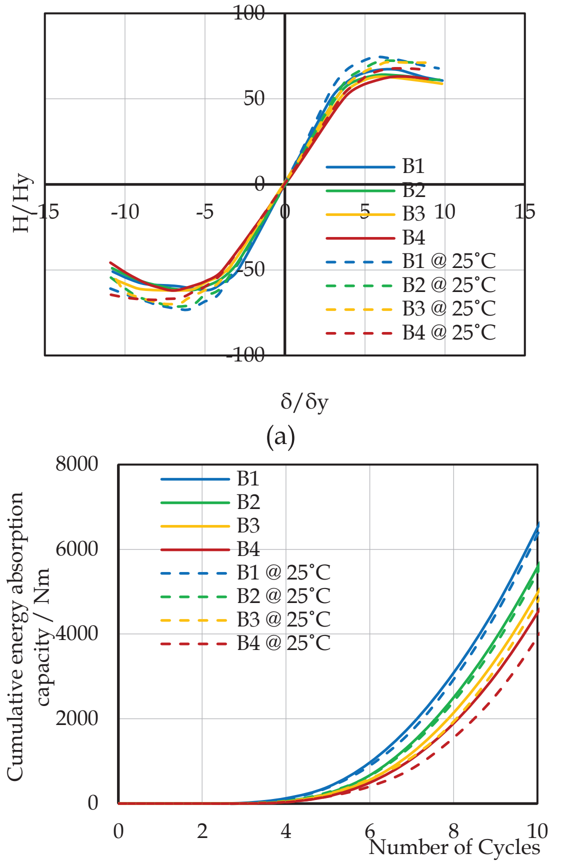

(b)

Figure 18 - Results of Case 2: (a) cyclic envelope curves and (b) cumulative energy curves

The maximum ductility and maximum strength curves were obtained by considering the cyclic envelope curves under fire condition of Case 2, and by considering cumulative energy absorption capacity curves the maximum accumulated energy absorption capacity was obtained, as indicated in Figure 19, where variation of each parameter was plotted against the middle bay beam flexural stiffness.

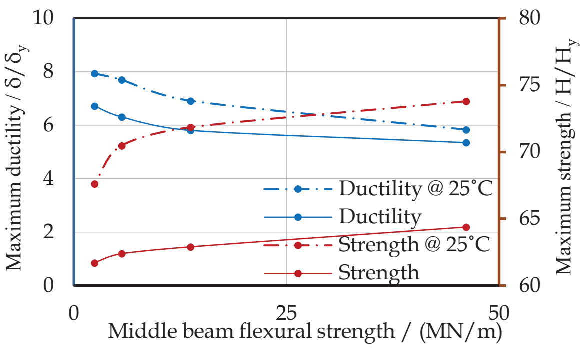

(a)

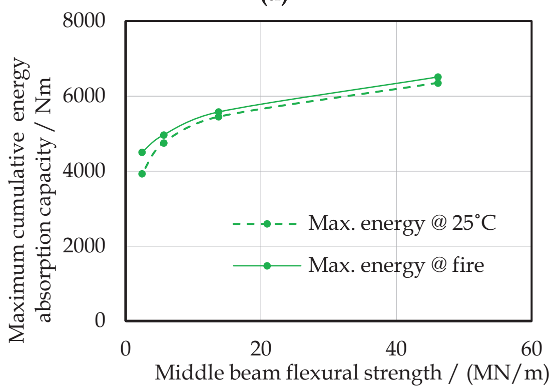

(b)

Figure 19 - Seismic parameters of Case 2: (a) maximum ductility and maximum strength variation and (b) maximum cumulative energy absorption capacity variation

The maximum ductility decreased and the maximum strength and maximum cumulative energy absorption capacity increased with increasing middle bay beam stiffness as indicated in Figure 19.

The reduction or incremental percentages of seismic parameters in Case 2 have been obtained as shown in Table 6.

Table 6 - Percentage variation of seismic parameters for Case 2

Fire subcase	**Reduction (-) or incremental (+) percentage (%)**		
	Maximum ductility	**Maximum strength**	**Maximum cumulative energy absorption capacity**
B1	-8.35	-12.75	+2.46
B2	-16.02	-12.45	+2.34
B3	-18.03	-11.47	+4.46
B4	-15.31	-8.75	+14.5

The highest reduction percentage value for the maximum ductility is obtained in case B3 where lowest value was obtained in case B1 which represents the highest middle bay beam stiffness. The reduction percentage of maximum strength was increased with increasing middle bay beam stiffness and, for maximum cumulative energy absorption capacity, highest increment was obtained for case B4 which represents the lowest middle bay beam stiffness.

5. Conclusions

This study evaluates the seismic performance of a 4-bay, 2-story hollow steel moment-resisting frame in combined fire and cyclic loading condition. Using *PyroSim* for fire simulations and *ABAQUS* for thermal and structural analysis it examined the response of a frame to combined cyclic loading and fire exposure. The analysis involved varying fire location and middle bay beam flexural stiffness to assess impacts on load-displacement behaviour. From this study, the following conclusions were obtained:

- The proposed simulation methodology for coupled fire-structure analysis can be utilized to obtain the thermo-mechanical behaviour of steel moment-resisting frames with hollow elements (columns and beams) under fire conditions.
- When fire location changes, the maximum strength reduction varies within a range 7.52-9.80%, the maximum ductility reduction 9.91-15.09% and the increment in maximum cumulative energy absorption capacity range 10.01-15.28% compared to room temperature (250C) response. It indicates highest ductility and strength reduction in case of fire at column next to cyclic loaded point while lowest energy absorption capacity in case of fire at column of cyclic loaded point.
- Fire at the second and fourth columns leads to more significant increases in energy absorption capacity and more pronounced reductions in strength when the cyclic load is applied at the top of the first column.
- When the beam stiffness was increased, strength reduction increased by 8.75-12.75%, ductility reduction increased by 8.35-18.03% and energy absorption varied within 2.34-14.5% compared to room temperature (250C) response. It can be observed that maximum strength, maximum energy and lowest ductility are obtained in highest middle bay beam flexural stiffness case which indicate higher stability.
- Maximum strength and the energy absorption capacity were increased and the ductility was reduced with the increase of middle bay beam stiffness.

Acknowledgement

The authors would like to express their appreciation for licensed applications of the *ABAQUS* package facilitated by the Finite Element Analysis and Simulation Centre, Rubber Research Institute of Sri Lanka, Ratmalana.

References

1. Duan, T., Chen, Y. and Lu, R. (2024) "Construction Technology of Steel Structures in Large Public Buildings." *ACETR*, 1, p.67. https://doi.org/10.61935/acetr.2.1.2024.P67

2. NCSTAR, N. (2005) 'Final Report on the Collapse of the World Trade Center Towers', *National Construction Safety Team for the Federal Building and Fire Safety Investigation of the World Trade Center Disaster*, *National Institute of Standards and Technology*, Gaithersburg, MD [Preprint].

3. Menéndez, E. and Vega, L. (2010) "Analysis of the Behaviour of the Structural Concrete after the Fire at the Windsor Building in Madrid", *Fire and Materials: An International Journal*, 34(2), pp. 95-107. https://doi.org/10.1002/fam.1013

4. Yamazaki, F. and Matsuoka, M. (2007) "Remote Sensing Technologies in Post-Disaster Damage Assessment." *Journal of Earthquake and Tsunami*, 1(03), pp. 193–210. https://doi.org/10.1142/S1793431107000122

5. DesRoches, R., Comerio, M., Eberhard, M., Mooney, W., Rix, G.J. (2011) "Overview of the 2010 Haiti Earthquake." *Earthquake Spectra* 27, 1–21. https://doi.org/10.1193/1.3630129

6. Simons, M., Minson, S.E., Sladen, A., Ortega, F., Jiang, J., Owen, S.E., Meng, L., Ampuero, J.-P., Wei, S., Chu, R. (2011) "The 2011 Magnitude 9.0 Tohoku-Oki Earthquake: Mosaicking the Megathrust from Seconds to Centuries." *science* 332, 1421–1425. https://doi.org/10.1126/science.1206731

7. European Committee for Standardization (CEN) (2005) *EN 1993-1-2: Eurocode 3: Design of steel structures – Part 1-2: General rules – Structural fire design*. Brussels: CEN.

8. European Committee for Standardization (CEN) (2004) *EN 1998-1: Eurocode 8: Design of structures for earthquake resistance – Part 1: General rules, seismic actions and rules for buildings*. Brussels: CEN.

9. Jiang, B., Li, G.-Q., Li, L., Izzuddin, B.A. (2018) "Experimental Studies on Progressive Collapse Resistance of Steel Moment Frames under Localized Furnace Loading." *J. Struct. Eng*. 144, 04017190. https://doi.org/10.1061/(ASCE)ST.1943-541X.0001947

10. Sakurahara, T., Reihani, S.A., Mohaghegh, Z., Brandyberry, M., Kee, E., Johnson, D., Rodgers, S., Billings, M.A. (2014) 'Developing a New Fire PRA Framework by Integrating Probabilistic Risk Assessment with a Fire Simulation Module', Presented at the *12th International Probabilistic Safety Assessment and Management Conference, PSAM 2014*.

11. Zehfuss, J., Hosser, D. (2007) "A Parametric Natural Fire Model for the Structural Fire Design of Multi-Storey Buildings." *Fire Safety Journal* 42, 115–126. https://doi.org/10.1016/j.firesaf.2006.08.004

12. Ralph, B., Carvel, R. (2018) "Coupled Hybrid Modelling in Fire Safety Engineering; A Literature Review." *Fire Safety Journal* 100, 157–170. https://doi.org/10.1016/j.firesaf.2018.08.008

13. Kleiber, M., Burczyński, T., Wilde, K., Gorski, J., Winkelmann, K., Smakosz, Ł. (Eds.) (2016) 'Advances in Mechanics: Theoretical, Computational and Interdisciplinary Issues' *Proceedings of the 3rd Polish Congress of Mechanics (PCM) and 21st International Conference on Computer Methods in Mechanics (CMM)*, Gdansk, Poland, 8-11 September 2015. CRC Press.

14. Franssen, J.-M., Real, P.V. (2016) *Fire Design of Steel Structures: EC1: Actions on structures; Part 1-2: Actions on structure exposed to fire; EC3: Design of steel structures; Part 1-2: Structural fire design*. John Wiley & Sons. https://doi.org/10.1002/9783433607008

15. Agarwal, A., Varma, A.H. (2014) "Fire Induced Progressive Collapse of Steel Building Structures: The Role of Interior Gravity Columns." *Engineering Structures* 58, 129–140. https://doi.org/10.1016/j.engstruct.2013.09.020

16. Venkatachari, S., Kodur, V.K.R. (2023) "Modeling Parameters for Predicting the Fire-Induced Progressive Collapse in Steel Framed Buildings." *Resilient Cities and Structures* 2, 129–144. https://doi.org/10.1016/j.rcns.2023.10.003

17. Jiang, B., Li, G.-Q., Li, L., Izzuddin, B.A. (2017) "Simulations on Progressive Collapse Resistance of Steel Moment Frames under Localized Fire." *Journal of Constructional Steel Research* 138, 380–388. https://doi.org/10.1016/j.jcsr.2017.05.018

18. Zhang, C., Silva, J.G., Weinschenk, C., Kamikawa, D., Hasemi, Y. (2016) "Simulation Methodology for Coupled Fire-Structure Analysis: Modeling Localized Fire Tests on a Steel Column." *Fire Technology* 52, 239–262. https://doi.org/10.1007/s10694-015-0495-9

19. Liu, Z., Silva, J.C.G., Huang, Q., Hasemi, Y., Huang, Y., Guo, Z. (2021) "Coupled CFD–FEM Simulation Methodology for Fire-Exposed Bridges." *J. Bridge Eng.* 26, 04021074. https://doi.org/10.1061/(ASCE)BE.1943-5592.0001770

20. Kallada Janardhan, R., Shakil, S., Lu, W., Hostikka, S. and Puttonen, J. (2022) "Coupled CFD-FE Analysis of a Long-Span Truss Beam Exposed to Spreading Fires." *Engineering Structures*, 259, p.114150. https://doi.org/10.1016/j.engstruct.2022.114150

21. Chen, C., Jiang, L., Qiu, J., Orabi, M.A., Chan, W.S. and Usmani, A. (2023) "Opensees Development for Modelling Timber Structural Members Subjected to Realistic Fire Impact." *Fire and Materials*, 47, pp.461–478. https://doi.org/10.1002/fam.3115

22. Rackauskaite, E., Kotsovinos, P. and Rein, G. (2017) "Model Parameter Sensitivity and Benchmarking of the Explicit Dynamic Solver of LS-DYNA for Structural Analysis in Case of Fire." *Fire Safety Journal*, 90, pp.123–138. https://doi.org/10.1016/j.firesaf.2017.03.002

23. Paajanen, A., Korhonen, T., Merja, S., Hostikka, S. and Malendowski, M. (2013) "FDS2FEM – A Tool for Coupling Fire and Structural Analyses', In: *IABSE Workshop, Helsinki 2013: Safety, Failures and Robustness of Large Structures*, Helsinki, Finland, pp.218–224. https://doi.org/10.2749/222137813807054629

24. Tran, V.-L., Thai, D.-K., Nguyen, D., Phan, H.-T., Nguyen, V.-Q. (2019) "Finite Element Simulation of Steel Beam under Fire."

25. European Committee for Standardization (CEN) (2005) *EN 1991-1-4: Eurocode 1: Actions on structures – Part 1-4: General actions – Wind actions*. Brussels: CEN.

26. Tateishi, K., Chen, T. and Hanji, T. (2008) "Extremely Low Cycle Fatigue Assessment Method for Un-Stiffened Cantilever Steel Columns." *Doboku Gakkai Ronbunshuu A*, 64, pp.288–296. https://doi.org/10.2208/jsceja.64.288

27. National Steel Standardization Technical Committee of China (1999) "Quality Carbon Structural Steels." *GB/T699-1999*, Beijing (in Chinese)

28. Seif, M. et al. (2016) Temperature-Dependent Material Modeling for Structural Steels: Formulation and Application. *NIST TN 1907*. National Institute of Standards and Technology, p. NIST TN 1907. https://doi.org/10.6028/NIST.TN.1907